Nature of optical excitations in the frustrated kagome compound herbertsmithite

A. Pustogow, Y. Li, I. Voloshenko, P. Puphal, C. Krellner, I. I. Mazin, M. Dressel, and R. Valentí

Phys. Rev. B **96**, 241114 — Published 29 December 2017

DOI: 10.1103/PhysRevB.96.241114

Nature of optical excitations in the frustrated kagome compound Herbertsmithite

A. Pustogow,[1] Y. Li,[2] I. Voloshenko,[1] P. Puphal,[3] C. Krellner,[3] I.I. Mazin,[4] M. Dressel,[1] and R. Valentí[2]

[1] *1. Physikalisches Institut, Universität Stuttgart, 70569 Stuttgart, Germany*
[2] *Institut für Theoretische Physik, Goethe-Universität Frankfurt, 60438 Frankfurt am Main, Germany*
[3] *Physikalisches Institut, Goethe-Universität Frankfurt, 60438 Frankfurt am Main, Germany*
[4] *Code 6393, Naval Research Laboratory, Washington, DC 20375, USA*

Optical conductivity measurements are combined with density functional theory calculations in order to understand the electrodynamic response of the frustrated Mott insulators Herbertsmithite $ZnCu_3(OH)_6Cl_2$ and the closely-related kagome-lattice compound $Y_3Cu_9(OH)_{19}Cl_8$. We identify these materials as charge-transfer rather than Mott-Hubbard insulators, similar to the high-T_c cuprate parent compounds. The band edge is at 3.3 and 3.6 eV, respectively, establishing the insulating nature of these compounds. Inside the gap, we observe dipole-forbidden local electronic transitions between the Cu 3*d* orbitals in the range 1–2 eV. With the help of *ab initio* calculations we demonstrate that the electrodynamic response in these systems is directly related to the role of on-site Coulomb repulsion: while charge-transfer processes have their origin on transitions between the ligand band and the Cu 3*d* upper Hubbard band, *local d-d* excitations remain rather unaffected by correlations.

Since the discovery of high-T_c cuprates, the physics of strongly correlated materials has been at the forefront of research in condensed matter physics. The relationship between correlations, unconventional superconductivity, quantum-spin-liquid behavior and other exotic states of matter has been intensely debated. While at the level of model theories one can introduce criteria to quantify the degree of correlation, such as the ratio U/W, where U is the on-site Coulomb repulsion and W is the single-particle bandwidth, the quantification in many materials is not that straightforward. The effect of correlations usually shows up as mass renormalization, band narrowing, or as opening or enhancement of the band gap[1,2].

Cu^{+2} ions are, arguably, the most strongly correlated among *d* transition metals[3–6]. They are key ingredients of high-T_c cuprates and have been widely investigated in the last decades. A recent revival of interest in Cu-based materials was triggered by the discovery of geometrically frustrated cuprates that seem to exhibit spin-liquid properties[7–16] and may even harbor unconventional superconductivity with higher angular momenta than existing superconductors[17] or further topological phases[18] although synthesis seems to be difficult[19].

In this work we investigate the origin of the optical excitations in the spin-liquid candidate Herbertsmithite and concentrate on the following conceptual issue: which measurable properties in correlated systems are strongly affected by correlation effects and which are not? We will show, experimentally and theoretically, that in a single experimental probe, namely optical conductivity, one can simultaneously observe properties dramatically influenced by Coulomb (Mott-Hubbard) correlation effects, and those that are hardly affected at all.

One can distinguish two types of optical absorption processes, depicted in Fig. 1. On the one hand, we have the "charge-transfer process", that in its simple form can be described as creating a hole and an electron residing at different lattice sites; the corresponding changes of charge distribution modify the Coulomb energy. The second process, usually referred to as local *d-d* transitions, creates an electron-hole pair residing on the same transition-metal site which, nominally, does not enhance the Hubbard repulsion. The main conceptual problem with this picture is that the notion, rigorously speaking, applies only to an isolated transition-metal ion — in which case any local transition between the *d*-orbitals is forbidden by symmetry[20–22]. One *can*, however, meaningfully apply the same nomenclature in an extended solid, but then it should refer to the one-electron propagator in real space that originates and ends on the same site, or on different sites. This way, any residual itinerancy can be formally incorporated into the concept. Note, while photoemission probes the self-energy of the single-particle Green

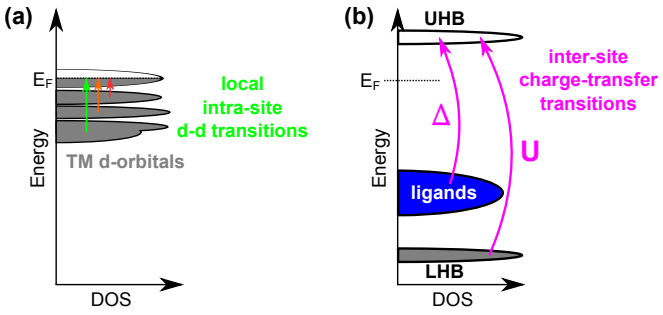

FIG. 1. (Color online) Two distinct types of inter-band excitations are identified in strongly correlated transition-metal (TM) compounds. (a) *Local* excitations between the *d*-orbitals on the same TM ion do not change the site charge and, hence, remain rather unaffected by electronic correlations. (b) Charge transfer processes between different sites change the local electron density and are, therefore, strongly affected by the on-site Coulomb interaction. While the charge-transfer gap Δ has to be overcome for excitation of an electron from the ligands to the upper Hubbard band (UHB) of the TM ion, the Coulomb repulsion U has to be paid for inter-site TM ion - TM ion charge transfer, corresponding to transitions between the Hubbard bands.

function and is described by diagrams changing the number of electrons, optical absorption is a polarization bubble (self-energy of the two-particle Green function) and, thus, always *conserves* the total number of particles in the system (but not necessarily on each site).

In this language, the problem of the dipole matrix elements solves itself automatically. In an extended solid, a Green function originating at a given transition-metal site is not necessarily localized on the same site. As long as the corresponding atomic state acquires dispersion, it always includes some admixture of "orbital tails" coming from other sites, primarily ligands, but not only. In density functional and similar calculations it is seen as admixture of other characters into formally d-bands. Now it is important to recognize that around each site, say, within the atomic sphere, electronic wave functions, no matter whether "native" or penetrating from outside, have to solve the radial Schrödinger equation for the "host" site. In other words, the tails of surrounding orbitals are re-expanded around the transition-metal site as a linear combination of the transition-metal s-, p-, d-, f- orbitals. Therefore, in optical calculations the so-called d-d excitations are treated as local, but the corresponding local states have admixture of other characters; the dipole transitions proceed between the main d portion of the angular-momentum-decomposed states and the minor admixture of p- and f- characters.

This is, in a nutshell, the physics we want to address. We have chosen herbertsmithite-type compounds, $ZnCu_3(OH)_6Cl_2$ and $Y_3Cu_9(OH)_{19}Cl_8$ as our testing ground, for the following reasons: (i) they have, as we will show, sizeable Mott-Hubbard correlation gaps of the order of 3 eV, and thus leave a window of transparency at lower energies where we expect the d-d excitations to manifest themselves; (ii) while intensively studied by magnetic and thermodynamic probes[7–10,14,23–29], optical investigations focused only on the low-energy excitations and phonons[30–32] and the details of the band structure of these materials have not been well characterized; even such basic parameters, extremely important for theoretical models, such as the Coulomb repulsion U and the hierarchy of the crystal field levels, have not been determined reliably in experiment so far. Hence, our goal is twofold: to fill a lacuna in the characterization of these intensely studied compounds and to gain insight into the physics of the local d-d optical excitations.

Single crystals of $ZnCu_3(OH)_6Cl_2$ and $Y_3Cu_9(OH)_{19}Cl_8$ were grown by hydrothermal methods. We reproduced the hydrothermal synthesis of several batches of Herbertsmithite single crystals following Ref. 35. $Y_3Cu_9(OH)_{19}Cl_8$ single crystals were synthesized hydrothermally following Ref. 29 using a duran glass ampoule in an autoclave heated to 270° C followed by slow cooling to 260° C. The optical reflectivity was measured on thick ($d > 0.4$ mm) samples, and for transmission measurements very thin ($10\ \mu\text{m} \lesssim d \lesssim 70\ \mu$m), plate-like crystals were selected. The experiments were performed with a Woollam ellipsometer covering

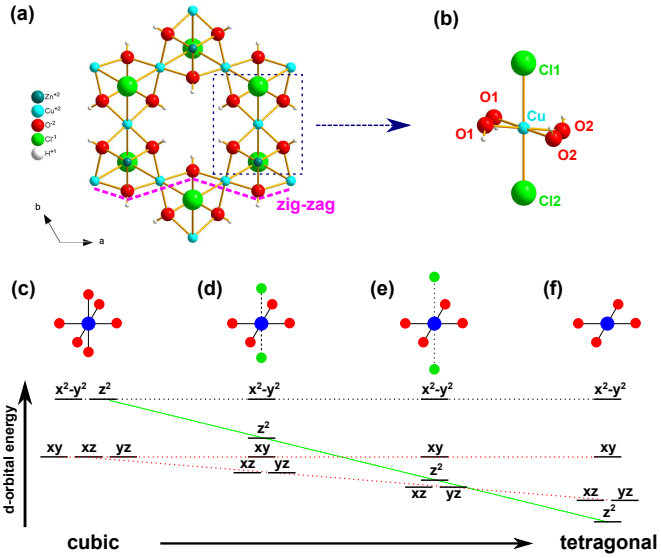

FIG. 2. (a) The crystal structure of $ZnCu_3(OH)_6Cl_2$ exhibits the characteristic kagome arrangement of Cu atoms[33]. (b) The CuO_4Cl_2 octahedra are strongly distorted as the Cl atoms are more distant from the center Cu site than the O atoms. In addition, the CuO_4 tetragon is tilted with respect to the equatorial plane perpendicular to the Cl-Cu-Cl axis, effectively flattening the zig-zag shape of the CuO chains with respect to the kagome layer. (c)-(f) Increasing the vertical distortion lowers the z^2 orbital relative to the x^2-y^2 state[34].

the frequency range 0.6 eV $< \hbar\omega <$ 6 eV. The transmission was probed at normal incidence only, while for ellipsometry reflection geometry with various angles of incidence was employed. In the visible range and at lower frequencies we performed additional measurements at normal incidence in a commercial Bruker Fourier-transform infrared spectrometer (0.005 eV $< \hbar\omega <$ 3 eV), confirming the transmission data in the overlapping range. We also calculated the optical conductivity from the broadband reflectivity using the Kramers-Kronig relation, verifying our ellipsometric results[36].

For the density functional theory (DFT) calculations we used the experimentally determined crystal structure of $ZnCu_3(OH)_6Cl_2$[33], and employed the linearized augmented plane-wave (LAPW) package WIEN2k[37] with the generalized gradient approximation (GGA)[38]. The basis-controlling parameter was set to $RK_{\max} = 3$ due to the presence of H in the structure. This value is equivalent to $RK_{\max} \sim 7-9$ for oxides. We used a mesh of 1000 **k** points in the first Brillouin zone (FBZ) of the primitive unit cell. The density of states (DOS) and hopping parameters were computed with $20 \times 20 \times 20$ **k** points in the full Brillouin zone for the GGA calculation. In order to address correlation effects in the charge-transfer processes, we used the GGA + U method in the spherically averaged approximation[39] and assumed various antiferromagnetic configurations (see Ref. 36). For DOS and optical conductivity GGA + U calculations, we have chosen 2340 **k** points in the primitive unit cell.

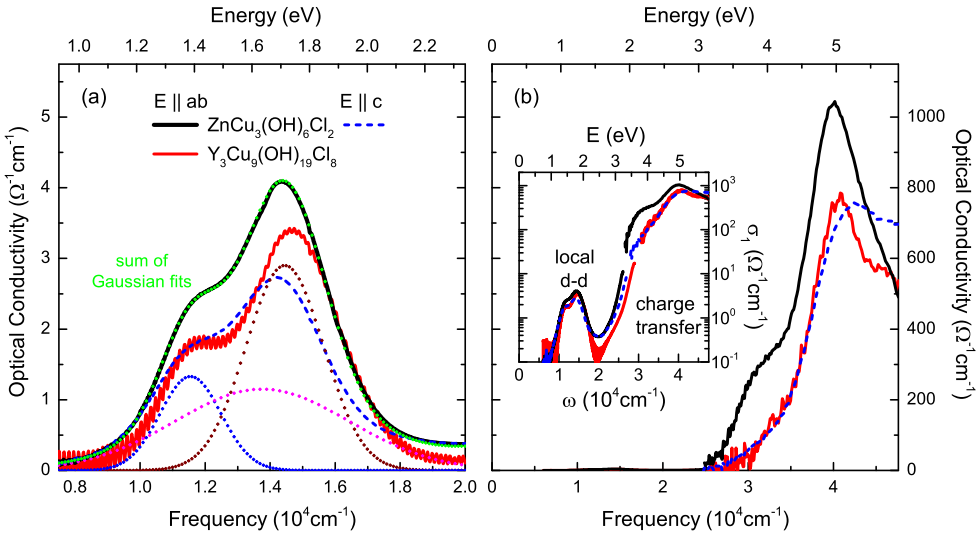

FIG. 3. The optical conductivity of $ZnCu_3(OH)_6Cl_2$ (solid black) and $Y_3Cu_9(OH)_{19}Cl_8$ (solid red) in the visible and ultraviolet range shows general similarity proving that the electrodynamics is mainly determined by the Cu kagome network. (a) We assign the weak low-frequency multi-peak to dipole-forbidden local transitions between the Cu $3d$ orbitals. One broad and two narrow Gaussians are necessary to satisfactorily fit the data (small symbols). For $ZnCu_3(OH)_6Cl_2$ crystal geometry also allowed to measure the out-of-plane conductivity (dashed blue), which has similar frequency dependence, but smaller intensity. (b) The strong high-frequency feature is identified as the charge transfer between ligands and the unoccupied Cu $3d$ states (upper Hubbard band). The inset illustrates the different intensity of local and charge-transfer processes on a logarithmic scale.

Fig. 2 shows the details of the Herbertsmithite structure. Each Cu^{+2} is surrounded by four O^{-2} and two more distant Cl^{-} anions, forming a distorted octahedron [Fig. 2(b)]. The interatomic distances are listed in Ref. 36. Chemical disparity between Cl and O implies a considerable tetragonal component in the crystal field. The Cu-Cl bond is significantly longer than the Cu-O one, even accounting for the larger radius Cl^{-}. Hence, in the simple ligand-field picture the e_g levels will split as x^2-y^2 (high) and z^2 (low), and the t_{2g} states as xy (high) and $\{xz, yz\}$ (low), as illustrated in Fig. 2 (c)-(f). In a real crystal, however, the arrangement of d-orbitals is hard to predict without actual calculations. Another effect of stretching the CuO_4Cl_2 octahedra is the tilt of the O_4 tetragon with respect to the equatorial plane perpendicular to the Cl-Cu-Cl axis. This tilting effectively straightens the Cu-O zig-zag chains oriented along a, b and $a+b$ and affects the bandwidth and band gap.

Fig. 3 displays the optical conductivity of $ZnCu_3(OH)_6Cl_2$ and $Y_3Cu_9(OH)_{19}Cl_8$ measured in the visible and ultraviolet ranges. Two distinct features are identified in the spectra of both compounds as it is common in Cu^{+2} systems[6,34,40–47]. While local d-d transitions appear around 1–2 eV, intense charge-transfer excitations set in above 3 eV, where the original hole of the Cu x^2-y^2 state is filled by an electron from the ligands, creating a hole on the ligands. To reproduce the latter process in standard *ab initio* calculations one has to include the effect of the Hubbard repulsion, which is done in the simplest mean-field way in the framework of the GGA + U formalism.

The optical conductivity shows an interesting structure: the absorption edge is around 3.3 and 3.6 eV for $ZnCu_3(OH)_6Cl_2$ and $Y_3Cu_9(OH)_{19}Cl_8$, respectively. This difference is likely due to different CuO_4 tiltings – $Y_3Cu_9(OH)_{19}Cl_8$ is closer to a rectangular arrangement than $ZnCu_3(OH)_6Cl_2$[36] – as discussed above. Contrasting the in- and out-of-plane polarizations of $ZnCu_3(OH)_6Cl_2$, we find significant anisotropy.

In Fig. 4 we present the DOS and optical conductivity obtained from GGA + U calculations with $U_{\rm eff} = U - J_H \approx 8$ eV which is a typical value for Cu^{+2}. J_H defines the Hund's rule coupling, usually 0.9–1 eV for $3d$ electrons. These results reproduce well the optical transitions observed above 3 eV in $ZnCu_3(OH)_6Cl_2$ [Fig. 3 (b)]. The dominant ligand character of the occupied states highest in energy in Fig. 4 (a) clearly establishes Herbertsmithite as a charge-transfer insulator with the spectral gap between the ligand band and the unoccupied Cu $3d$ band. The large Cu contributions below $E-E_F \approx -4$ eV correspond to the lower Hubbard band. In particular, we can identify the gap of 3.4 eV, a shoulder at 4 eV (4–4.6 eV in the calculations) and the strong ascend at 5 eV (5–5.5 in the calculations). Even the experimental anisotropy is well reproduced. In our calculation, the antiferromagnetic configuration introduces in-plane anisotropy between σ_{yy} (y is along b) and σ_{xx} (x is perpendicular to b), we averaged these to obtain $\sigma_{ab} = (\sigma_{xx}+\sigma_{yy})/2$[36]. The origin of the transitions can be traced back to the DOS as shown in Fig. 4 (a). Note that in the LAPW calculations there are considerable interstitial contributions to the DOS. The small

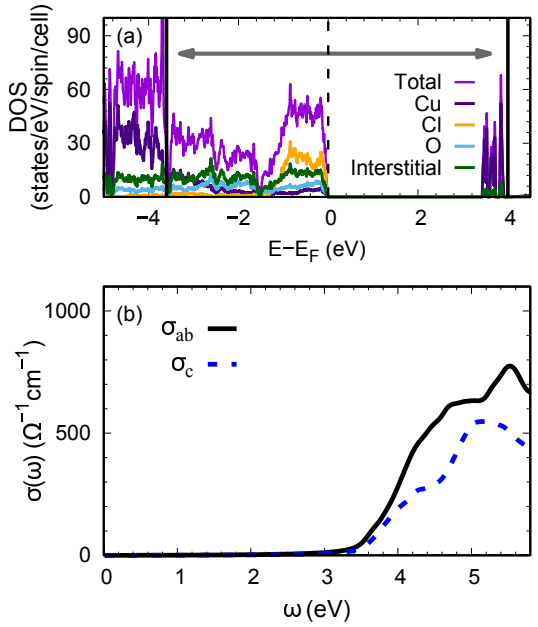

FIG. 4. (a) Density of states (DOS) and (b) optical conductivity for in- (σ_{ab}) and out-of-plane (σ_c) directions of $ZnCu_3(OH)_6Cl_2$ calculated by GGA + U. It reproduces the charge-transfer gap observed in experiment for $U_{\rm eff} = U - J_H = 8$ eV. The arrow in (a) indicates the energy range we considered to calculate $\sigma(\omega)$ in (b). The gap of 3.4 eV and main peaks around 5 eV coincide with the data in Fig. 3 (b).

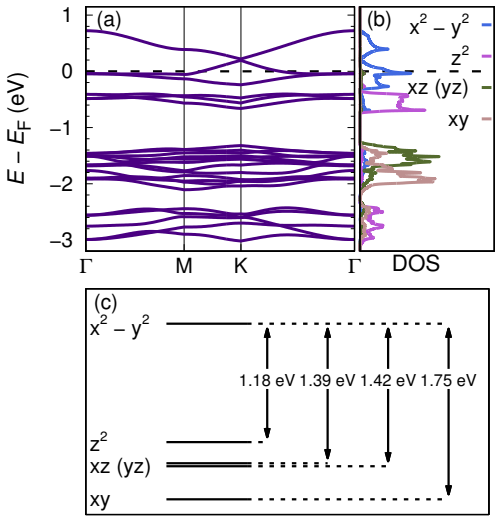

FIG. 5. Calculated GGA (a) band structure and (b) Cu 3d orbital resolved density of states (DOS) for $ZnCu_3(OH)_6Cl_2$ at $U = 0$. (c) Energy level diagram for on-site Cu 3d orbitals. The energy differences of the three levels 1.18 eV, 1.39 eV and 1.42 eV correspond to the experimental peaks in Fig. 3 (a).

O-H distance requires the use of small RMT (1.01 Å) in the calculation, implying that oxygen states reach into the interstitials. We can identify the optical processes as charge transfer transitions from ligands p states to the Cu 3d upper Hubbard band. The arrow between -3.6 eV and 4 eV in Fig. 4 (a) indicates the energy region considered for the optical conductivity calculations.

Now we turn our attention to the measured local *dipole-forbidden d-d* low energy excitations, displayed in Fig. 3 (a), which appear *inside* the charge transfer gap (inset panel b). They are visible in the experiment as a double peak around 1–2 eV causing the blue-green color of the $ZnCu_3(OH)_6Cl_2$ and $Y_3Cu_9(OH)_{19}Cl_8$ crystals. The intensity is small since, as discussed above, these transitions are only possible because the ligand orbitals penetrate the vicinity of the Cu site and get re-expanded into the $l = 1$ and $l = 3$ harmonics. This is corroborated by our calculations which reveal that the Cu d states are mixed with O and Cl p states (see Ref. 36). The experimental data can be satisfactorily fitted by three Gaussians, as indicated for $ZnCu_3(OH)_6Cl_2$ by the blue, magenta and wine curves in Fig. 3 (a). In order to understand the origin of these peaks, we need information of the crystal field splitting in the extended crystal. This can be accurately obtained by GGA calculations as shown in Fig. 5 (a) and (b). We obtain the following band order: $x^2 - y^2$, z^2, xz (yz), xy. We find that while the xy and the $\{xz, yz\}$ states are very close in energy, their order is reversed, the xy being lower; this indicates that the simple ligand-field model sketched in Fig. 2 (c)-(f) is an oversimplification. We then calculate the on-site and hopping parameters using the projector method described in Refs.[48,49]. For that, due to the strong hybridization of Cu with Cl, we consider 23 bands including Cu d, Cl p and Zn e_g orbitals[36,50]. The diagonalized on-site hopping matrix elements after shifting the energy of the unoccupied $x^2 - y^2$ state to 0 are -1.18 eV, -1.39 eV, -1.42 eV and -1.75 eV, with the dominant characters as described above. We find overall a very good agreement of the level positions with the multipeak structure of the observed local d-d transitions. We note that in the context of other transition-metal compounds, the origin of these transitions has been intensively debated, and other effects than the above discussed mixing of states such as phonons, magnons and spin-orbit coupling have been also suggested to contribute to making 'allowed' the dipole-forbidden d-d transition[20–22,47,51]. In our case we can explain the main features in terms of mixing of states in the tetragonally distorted CuO_4Cl_2 octahedra together with vibronic coupling. The effect of phonons is revealed as a narrowing and blue-shift of the absorption bands upon cooling[20–22]; the temperature dependence of the local d-d transitions is discussed in Ref.[36].

In this regard, we associate the lowest energy feature observed in experiment to transitions from z^2 to $x^2 - y^2$ while the slightly higher energy processes correspond to transitions from t_{2g} states to $x^2 - y^2$. The broad Gaussian peak in Fig. 3 (a) can be associated to the fact that the $\{xz, yz\}$ levels are almost degenerate as we show in Fig. 5 (c), in addition to temperature effects. Although calculated only for $ZnCu_3(OH)_6Cl_2$, the similarity of optical

spectra suggests likewise results for $Y_3Cu_9(OH)_{19}Cl_8$.

To conclude, with this study we unveil the nature of optical excitations in the frustrated kagome-lattice Mott insulators $ZnCu_3(OH)_6Cl_2$ and $Y_3Cu_9(OH)_{19}Cl_8$ by means of optical spectroscopy and density functional theory calculations. We identify the edge of the charge-transfer band at 3.3 and 3.6 eV in the experimental spectra, respectively, in good agreement with calculations corresponding to transitions from the ligand states to the Cu-*d* upper Hubbard band with an on-site Coulomb interaction of 8 eV. Inside the gap, we observe dipole-forbidden *d*-*d* transitions with small intensity. These local excitations imply only minor changes of the on-site charge and remain, therefore, rather unaffected by correlation effects. We thus identify a general route how to handle electronic correlations in theoretical calculations of optical excitations. Specifically, on-site Coulomb repulsion U is essential to describe the charge transfer process while it plays almost no role for local excitations. Finally, our findings demonstrate that the electrodynamic response of Herbertsmithite and its analogues is similar in nature to the parent compounds of high-T_c cuprates, being charge-transfer rather than Mott insulators[4,6,34,46].

ACKNOWLEDGMENTS

The project was supported by the Deutsche Forschungsgemeinschaft (DFG) through grants SFB/TR 49. I.I.M. was supported by A. von Humboldt foundation and by ONR through the NRL basic research program. A.P. and Y.L. equally contributed to this work.

[1] D. N. Basov, R. D. Averitt, D. van der Marel, M. Dressel, and K. Haule, Rev. Mod. Phys. **83**, 471 (2011).
[2] M. Imada, A. Fujimori, and Y. Tokura, Rev. Mod. Phys. **70**, 1039 (1998).
[3] J. Zaanen, G. A. Sawatzky, and J. W. Allen, Phys. Rev. Lett. **55**, 418 (1985).
[4] J. Zaanen and G. A. Sawatzky, J. Solid State Chem. **88**, 8 (1990).
[5] A. E. Bocquet, T. Mizokawa, T. Saitoh, H. Namatame, and A. Fujimori, Phys. Rev. B **46**, 3771 (1992).
[6] P. Olalde-Velasco, J. Jiménez-Mier, J. D. Denlinger, Z. Hussain, and W. L. Yang, Phys. Rev. B **83**, 241102 (2011).
[7] J. S. Helton, K. Matan, M. P. Shores, E. A. Nytko, B. M. Bartlett, Y. Yoshida, Y. Takano, A. Suslov, Y. Qiu, J.-H. Chung, D. G. Nocera, and Y. S. Lee, Phys. Rev. Lett. **98**, 107204 (2007).
[8] S.-H. Lee, H. Kikuchi, Y. Qiu, B. Lake, Q. Huang, K. Habicht, and K. Kiefer, Nat. Mater. **6**, 853 (2007).
[9] P. Mendels, F. Bert, M. A. de Vries, A. Olariu, A. Harrison, F. Duc, J. C. Trombe, J. S. Lord, A. Amato, and C. Baines, Phys. Rev. Lett. **98**, 77204 (2007).
[10] M. A. de Vries, K. V. Kamenev, W. A. Kockelmann, J. Sanchez-Benitez, and A. Harrison, Phys. Rev. Lett. **100**, 157205 (2008).
[11] P. A. Lee, Science **321**, 1306 (2008).
[12] L. Balents, Nature **464**, 199 (2010).
[13] P. Mendels and F. Bert, J. Phys. Soc. Jpn. **79**, 11001 (2010).
[14] T.-H. Han, J. S. Helton, S. Chu, D. G. Nocera, J. A. Rodriguez-Rivera, C. Broholm, and Y. S. Lee, Nature **492**, 406 (2012).
[15] M. Norman, Rev. Mod. Phys. **88**, 041002 (2016).
[16] L. Savary and L. Balents, Rep. Prog. Phys. **80**, 016502 (2017).
[17] I. I. Mazin, H. O. Jeschke, F. Lechermann, H. Lee, M. Fink, R. Thomale, and R. Valentí, Nat. Commun. **5**, 4261 (2014).
[18] D. Guterding, H. O. Jeschke, and R. Valentí, Sci. Rep. **6**, 25988 (2016).
[19] Z. Kelly, M. Gallagher, and T. McQueen, Phys. Rev. X **6**, 41007 (2016).
[20] A. B. P. Lever, *Inorganic electronic spectroscopy* (Elsevier, Amsterdam, 1968).
[21] R. G. Burns, *Cambridge Topics in Mineral Physics and Chemistry*, 2nd ed. (Cambridge University Press, Cambridge, 1993).
[22] E. I. Solomon and A. B. P. Lever, *Inorganic electronic structure and spectroscopy* (Wiley & Sons, Inc., 1999) pp. 213–258.
[23] A. Olariu, P. Mendels, F. Bert, F. Duc, J. C. Trombe, M. A. de Vries, and A. Harrison, Phys. Rev. Lett. **100**, 87202 (2008).
[24] A. Zorko, S. Nellutla, J. van Tol, L. C. Brunel, F. Bert, F. Duc, J.-C. Trombe, M. A. de Vries, A. Harrison, and P. Mendels, Phys. Rev. Lett. **101**, 26405 (2008).
[25] M. A. de Vries, J. R. Stewart, P. P. Deen, J. O. Piatek, G. J. Nilsen, H. M. Rønnow, and A. Harrison, Phys. Rev. Lett. **103**, 237201 (2009).
[26] J. S. Helton, K. Matan, M. P. Shores, E. A. Nytko, B. M. Bartlett, Y. Qiu, D. G. Nocera, and Y. S. Lee, Phys. Rev. Lett. **104**, 147201 (2010).
[27] T. Han, S. Chu, and Y. S. Lee, Phys. Rev. Lett. **108**, 157202 (2012).
[28] A. Zorko, M. Herak, M. Gomilšek, J. van Tol, M. Velázquez, P. Khuntia, F. Bert, and P. Mendels, Phys. Rev. Lett. **118**, 17202 (2017).
[29] P. Puphal, M. Bolte, D. Sheptyakov, A. Pustogow, K. Kliemt, M. Dressel, M. Baenitz, and C. Krellner, J. Mater. Chem. C **5**, 2629 (2017).
[30] M. A. de Vries, D. Wulferding, P. Lemmens, J. S. Lord, A. Harrison, P. Bonville, F. Bert, and P. Mendels, Phys. Rev. B **85**, 14422 (2012).
[31] D. V. Pilon, C. H. Lui, T. H. Han, D. Shrekenhamer, A. J. Frenzel, W. J. Padilla, Y. S. Lee, and N. Gedik, Phys. Rev. Lett. **111**, 127401 (2013).
[32] A. B. Sushkov, G. S. Jenkins, T.-H. Han, Y. S. Lee, and D. H. D, J. Phys.: Condens. Matter **29**, 95802 (2017).
[33] M. P. Shores, E. A. Nytko, B. M. Bartlett, and D. G. Nocera, J. Am. Chem. Soc. **127**, 13462 (2005).
[34] M. M. Sala, V. Bisogni, C. Aruta, G. Balestrino, H. Berger, N. B. Brookes, G. M. de Luca, D. D. Castro, M. Grioni, M. Guarise, P. G. Medaglia, F. M. Granozio, M. Minola, P. Perna, M. Radovic, M. Salluzzo, T. Schmitt, K. J.

Zhou, L. Braicovich, and G. Ghiringhelli, New J. Phys. **13**, 043026 (2011).
[35] T. H. Han, J. S. Helton, S. Chu, A. Prodi, D. K. Singh, C. Mazzoli, P. Müller, D. G. Nocera, and Y. S. Lee, Phys. Rev. B **83**, 100402 (2011).
[36] See Supplemental Material [url], which includes Refs. [52-59].
[37] P. Blaha, K. Schwarz, G. K. H. Madsen, D. Kvasnicka, and J. Luitz, WIEN2k, An Augmented Plane Wave Plus Local Orbitals Program for Calculating Crystal Properties (Karlheinz Schwarz, Techn. Universität Wien, Austria) (2001).
[38] J. P. Perdew, K. Burke, and M. Ernzerhof, Phys. Rev. Lett. **77**, 3865 (1996).
[39] V. I. Anisimov, I. V. Solovyev, M. A. Korotin, M. T. Czyżyk, and G. A. Sawatzky, Phys. Rev. B **48**, 16929 (1993).
[40] M. J. Riley, L. Dubicki, G. Moran, E. R. Krausz, and I. Yamada, Inorg. Chem. **29**, 1614 (1990).
[41] J. D. Perkins, J. M. Graybeal, M. A. Kastner, R. J. Birgeneau, J. P. Falck, and M. Greven, Phys. Rev. Lett. **71**, 1621 (1993).
[42] M. Bassi, P. Camagni, R. Rolli, G. Samoggia, F. Parmigiani, G. Dhalenne, and A. Revcolevschi, Phys. Rev. B **54**, R11030 (1996).
[43] J. D. Perkins, R. J. Birgeneau, J. M. Graybeal, M. A. Kastner, and D. S. Kleinberg, Phys. Rev. B **58**, 9390 (1998).
[44] C. de Graaf and R. Broer, Phys. Rev. B **62**, 702 (2000).
[45] S.-J. Hwu, M. Ulutagay-Kartin, J. A. Clayhold, R. Mackay, T. A. Wardojo, C. J. O'Connor, and M. Krawiec, J. Am. Chem. Soc. **124**, 12404 (2002).
[46] R. V. Pisarev, V. V. Pavlov, A. M. Kalashnikova, and A. S. Moskvin, Phys. Rev. B **82**, 224502 (2010).
[47] R. V. Pisarev, A. M. Kalashnikova, O. Schöps, and L. N. Bezmaternykh, Phys. Rev. B **84**, 75160 (2011).
[48] M. Aichhorn, L. Pourovskii, V. Vildosola, M. Ferrero, O. Parcollet, T. Miyake, A. Georges, and S. Biermann, Phys. Rev. B **80**, 085101 (2009).
[49] K. Foyevtsova, H. O. Jeschke, I. I. Mazin, D. I. Khomskii, and R. Valentí, Phys. Rev. B **88**, 035107 (2013).
[50] K. Riedl, Private communication.
[51] M. W. Haverkort, A. Tanaka, L. H. Tjeng, and G. A. Sawatzky, Phys. Rev. Lett. **99**, 257401 (2007).
[52] D. B. Tanner, Phys. Rev. B **91**, 35123 (2015).
[53] H. Fujiwara, *Spectroscopic Ellipsometry* (John Wiley & Sons, Ltd, Chichester, UK, 2007).
[54] K. Mereiter, ICSD Collection Code 425835 (2013).
[55] R. H. Colman, C. Ritter, and A. S. Wills, Chem. Mat. **20**, 6897 (2008).
[56] J. P. Perdew and M. Levy, Phys. Rev. Lett. **51**, 1884 (1983).
[57] L. J. Sham and M. Schlüter, Phys. Rev. Lett. **51**, 1888 (1983).
[58] I. I. Mazin and R. E. Cohen, Ferroelectrics **194**, 263 (1997).
[59] I. I. Mazin, E. Maksimov, S. Rashkeev, and Y. Uspenskii, J. Exp. Theor. Phys. **63**, 637 (1986).